

# Multifractal characteristics of particle size distributions (50–200 m) in soils in the vadose zone on the Loess Plateau, China

Jiangbo Qiao<sup>a</sup>, Yuanjun Zhu<sup>a,\*</sup>, Xiaoxu Jia<sup>b</sup>, Ming'an Shao<sup>a,b,c</sup>

<sup>a</sup> State Key Laboratory of Soil Erosion and Dryland Agriculture on the Loess Plateau, Northwest A&F University, Yangling, 712100, China

<sup>b</sup> Key Laboratory of Ecosystem Network Observation and Modeling, Institute of Geographic Sciences and Natural Resources Research, Chinese Academy of Sciences, Beijing, 100101, China

<sup>c</sup> College of Resources and Environment, University of Chinese Academy of Sciences, Beijing, 100190, China

## ARTICLE INFO

### Keywords:

Deep loess soil  
Fractal theory  
The Loess Plateau  
Particle size distribution  
Vadose zone

## ABSTRACT

The soil particle size distribution (PSD) is an important and basic physical property that determines many other chemical, physical, and biological properties of soil. Thus, quantitatively characterizing the soil PSD is important. However, the PSDs have not been characterized previously in deep soil profiles on the Loess Plateau, China. Therefore, in the present study, we employed single fractal theory and multifractal theory to quantitatively characterize these PSDs. Soil samples (50–200 m) were collected from the top of the soil profile down to the bedrock by drilling at five sites on the Loess Plateau in China. The results showed that the sand content had the highest coefficient of variation (CV) whereas the silt content had the lowest CV. Single fractal dimension (D) analysis detected significant positive relationships between D and the silt and clay contents, but a significant negative relationship with the sand content. Multifractal analysis indicated that the capacity dimension ( $D_0$ ) values at five sites tended to increase from south to north, whereas a decreasing trend was determined for the information dimension/capacity dimension ( $D_1/D_0$ ). Yangling had the lowest  $\Delta\alpha$  and  $\Delta D$  values, whereas Ansai had the highest. The  $\Delta f$  values were highest at Ansai and Shenmu. Our results are important to understand the soil physical properties and to estimate the soil hydraulic properties in deep profiles on the Loess Plateau.

## 1. Introduction

The soil particle size distribution (PSD) is an important and basic physical property, which can influence water movement, soil erosion, and vegetation productivity (Huang and Zhang, 2005; Peng et al., 2014). The PSD is also an important parameter for estimating the hydraulic properties of soil (e.g., soil water retention curve and soil saturated hydraulic conductivity) and bulk density (Filgueira et al., 2006; Hollis et al., 2012; Hwang et al., 2011). In addition, changes in the PSD can be used as indicators of the soil pedogenic intensity and formation processes (Minasny et al., 2016). Therefore, quantitatively characterizing the PSD is very useful in soil science.

At present, soil texture analysis is the most commonly used method for describing the PSD, which is considered one of the key soil properties that influence many other soil properties, such as the soil texture and soil infiltration (Keller and Dexter, 2012; Jones, 1983). However, soil texture analysis may be inadequate because the size definitions for the three particle fractions (clay, silt, sand) are rather arbitrary, thereby leading to incomplete soil PSD information (Wang et al., 2008). In order

to avoid the shortcomings of soil texture analysis, fractal theory has been used to characterize the PSD at multiple spatiotemporal scales (Peng et al., 2014). In particular, single fractal and multifractal theory have been applied to study the soil PSD (Gao et al., 2014; Xu et al., 2013; Sun et al., 2018). For example, Wang et al. (2008) described the multifractal characteristics of the PSDs for different land-use types on the Loess Plateau and found that multifractal parameters could potentially reflect the effects of land use on the soil physical properties and soil quality. Zhao et al. (2016) investigated the spatial variability of the soil PSD by applying fractal theory and geostatistical methods, and found that D might be a good indicator of soil erosion in their study area. Rodríguez-Lado and Lado (2017) showed that the entropy dimension ( $D_1$ ) was the best multifractal parameter for explaining the relationship between soil-forming factors and several multifractal parameters based on the PSDs for soils in Galicia, Spain. However, most of these previous studies focused on the PSDs in the upper soil layers and little information has been reported about the characteristics of the PSDs in deep soil profiles.

The Loess Plateau in China is located in the continental monsoon

\* Corresponding author.

E-mail address: [zhuyuanjun@foxmail.com](mailto:zhuyuanjun@foxmail.com) (Y. Zhu).

<https://doi.org/10.1016/j.still.2020.104786>

Received 14 April 2020; Received in revised form 17 July 2020; Accepted 10 August 2020

Available online 01 September 2020

0167-1987/ © 2020 Elsevier B.V. All rights reserved.

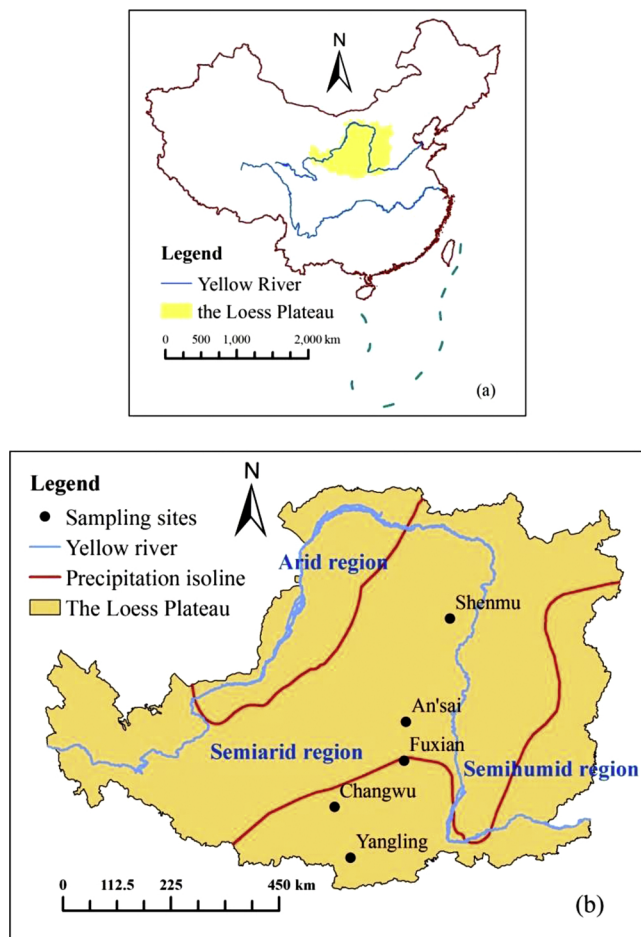


Fig. 1. Locations of (a) the Loess Plateau region in China and (b) the sampling sites.

region, and two-thirds of this region comprises arid or semiarid areas (Liu, 1985). The calculated mean thickness of the loess on the Loess Plateau is 105.7 m (Zhu et al., 2018), which makes it difficult to directly obtain soil moisture characteristics and hydraulic conductivities in deep profiles. Accurate characterization of the PSDs is required to estimate the hydraulic properties and bulk density in deep profiles on the Loess Plateau. In addition, detailed descriptions of the PSDs in the deep soil layer on the Loess Plateau would help for understanding the soil-forming processes. Thus, it is necessary to quantitatively characterize the PSDs in deep profiles on the Loess Plateau.

Therefore, the objectives of the present study were: (i) to investigate the vertical PSDs in deep profiles on the Loess Plateau; and (ii) to characterize the PSDs in deep profiles using single fractal and multifractal theory.

## 2. Materials and methods

### 2.1. Study area

The present study was conducted in the Loess Plateau region of China (33°43′–41°16′N, 100°54′–114°33′E) (Fig. 1a), which has a continental monsoon climate. In this region, the annual precipitation ranges from 150 mm in the northwest to 800 mm in the southeast, and 55–78% of the precipitation falls from June to September (Shi and Shao, 2000). The annual temperature ranges from 3.6 °C in the northwest to 14.3 °C in the southeast, and the annual evaporation in the Loess Plateau region is 1400–2000 mm. The vegetation zones in order from the southeast to the northwest comprise forest, forest-steppe,

typical-steppe, desert-steppe, and steppe-desert zones (Wang et al., 2013). The thickness of the soil on the Loess Plateau ranges from 30 m to 200 m, and the calculated average thickness is 105.7 m (Zhu et al., 2018).

### 2.2. Soil sampling

Five typical sampling sites were selected for collecting soil samples ranging from south to north in the Loess Plateau region, where they covered different vegetation types and climate zones (Fig. 1b). In addition, all of the sampling sites were selected at the summit positions in the landscape in order to ensure that the loess deposits were thick and complete, and they were located on flat ground in order to avoid significant soil erosion. Drilling equipment (assembled by Xi'an Qinyan Drilling Co., China) was used to extract soil samples from the soil surface to the bedrock. The soil samples were collected at 1-m intervals (0.5, 1.5, 2.5, 3.5 m, ...). Disturbed soil samples were collected to measure the PSD. Sampling was conducted from April to June in 2016.

### 2.3. Laboratory analysis

The disturbed soil samples were air dried, divided, and passed through 2-mm sieves. The soil PSD was determined using the laser diffraction method (Mastersizer 2000, Malvern Instruments, Malvern, UK) (Liu et al., 2005). Before acquiring the measurements, hydrogen peroxide was added to remove any soil organic matter and sodium hexametaphosphate was then used to disperse the soil samples. According to the soil taxonomy of the US Department of Agriculture (USDA), the PSD was divided into three components comprising the clay (< 0.002 mm), silt (0.002–0.05 mm), and sand (0.05–2 mm) contents.

### 2.4. Fractal theory

#### 2.4.1. Single fractal theory

The fractal dimension (D) of the soil PSD was estimated based on the volumetric distribution of the soil particle sizes (Gui et al., 2009) with the following equation:

$$\frac{V(r < R)}{V_T} = \left(\frac{R}{\lambda_V}\right)^{3-D}, \quad (1)$$

where  $r$  is the soil particle size (mm),  $V(r < R)$  is the cumulative volume of particles with a particle size smaller than  $R$  (where the volume is the percentage volume),  $V_T$  is the total volume of soil particles,  $\lambda_V$  is the upper limit for all fractions, which is numerically equal to the maximum particle size (mm),  $D$  is the soil fractal dimension, and  $V(r < R)/V_T$  is the cumulative volume percentage of soil particles with a particle size smaller than  $R$ . In the calculations,  $R$  was taken as the arithmetic mean of the upper and lower limits of a certain level.

#### 2.4.2. Multifractal theory

The particle size interval comprising  $I = [0.02, 2000]$  was obtained using the laser diffraction method, where  $I$  represents the logarithmic increase in the particle size. The interval  $I$  was divided into 64 cells of  $I = [\phi_i, \times_{i+1}]$ , where  $\phi_i$  represents the particle size in the measured sample. In order to analyze the PSD characteristics by multifractal theory, a dimensionless interval was established with an equal length subinterval. The value of  $\lg(\phi_{i+1}/\phi_i)$  is a constant, so the dimensionless interval of  $J = [\lg(0.02/0.02), \lg(2000/0.02)]$  was obtained. The interval for  $J = [0, 5]$  was then divided into equal length subintervals of  $N(\epsilon) = 2k$  ( $\epsilon = 5 \cdot 2^{-k}$ ). In order to ensure that each subinterval ( $J_i$ ) contained at least one measured value,  $k$  was set as equal to 1, 2, 3, 4, 5, and 6, and the corresponding values of  $\epsilon$  were 2.5, 1.25, 0.625, 0.3125, 0.15625, and 0.078125, respectively (Montero, 2005). Multifractal measures can also be described by scaling the  $q$ th moments of  $[Pi]$  distributions with the expression:

$$\mu_i(q, \epsilon) = \frac{\mu_i(\epsilon)^q}{\sum_{i=1}^{N(\epsilon)} P_i(\epsilon)^q}, \quad (2)$$

where  $\mu_i(q, \epsilon)$  is the q-order probability of the ith subinterval in J and q is the integer real number in the [-10,10] interval.

The formulae used to calculate the multifractal generalized dimension D (q) are as follows (Montero, 2005).

$$D(q) = \frac{1}{q-1} \lim_{\epsilon \rightarrow 0} \frac{\lg[\sum_{i=1}^{N(\epsilon)} P_i(\epsilon)^q]}{\lg \epsilon} \quad (q \neq 1) \quad (3)$$

$$D_1 = \lim_{\epsilon \rightarrow 0} \frac{\sum_{i=1}^{N(\epsilon)} P_i(\epsilon)^q \lg P_i(\epsilon)}{\lg \epsilon} \quad (q = 1) \quad (4)$$

The Rényi dimension D(q) reflects the overall multifractal characteristics. When  $q < 0$ , the information about the small probability distribution for sediment components is amplified. When  $q > 0$ , the information about the high probability distribution is amplified. When  $q = 0$ ,  $D_0$  is the capacity dimension representing the range of a continuous distribution, where the distribution range is wider when  $D_0$  is higher (Lyu et al., 2015). When  $q = 1$ ,  $D_1$  is the information entropy dimension representing the concentration of PSD, where the size distribution is more dispersive when  $D_1$  is higher (Wang et al., 2008). When  $q = 2$ ,  $D_2$  is the correlation dimension representing the uniformity of the measurement interval for the soil particle size, where the measurement interval is more uniform when  $D_2$  is higher (Miranda et al., 2006).

The equations used to calculate the multifractal singularity index  $\alpha(q)$  and singularity spectrum  $f(\alpha)$  are as follows.

$$\alpha(q) = \lim_{\epsilon \rightarrow 0} \frac{\sum_{i=1}^{N(\epsilon)} \mu_i(q, \epsilon) \lg P_i(\epsilon)}{\lg \epsilon} \quad (5)$$

$$f(\alpha(q)) = \lim_{\epsilon \rightarrow 0} \frac{\sum_{i=1}^{N(\epsilon)} \mu_i(q, \epsilon) \lg \mu_i(q, \epsilon)}{\lg \epsilon} \quad (6)$$

$\alpha(q)$  and  $f(\alpha(q))$  reflect the local branch multifractal characteristics.  $\alpha(0)$  is the mean value of the singular spectrum function, which is inversely proportional to the local density of the particle size fractal structure.  $\Delta\alpha = \alpha(q)_{\max} - \alpha(q)_{\min}$  represents the difference and inhomogeneity of the whole fractal structure, where the PSD is more uneven when  $\Delta\alpha$  is larger.  $\Delta f = f(\alpha_{\min}) - f(\alpha_{\max})$  represents the shape characteristics of the multifractal spectrum. When  $\Delta f < 0$ , the shapes of the singularity spectra deviate to the left and the small probability subsets of the soil PSD play major roles, thereby accounting for a smaller proportion of the volume fraction for the soil particles. When  $\Delta f > 0$ , the shapes of the singularity spectra deviated to the right and the large probability subsets of the soil PSD play major roles.

### 2.5. Statistical analysis

Microsoft EXCEL 2013 and MATLAB (version R2009a) were used for data analysis. All the statistical analysis were conducted using SPSS Version 16.0. One-way analysis of variance was conducted to determine the significance of the differences among the multifractal characteristic parameters at different sampling sites by using the least significant difference method. Pearson's correlation coefficients were calculated to analyze the correlations between the multifractal characteristic parameters and soil physicochemical properties at the 0.05 and 0.01 levels.

## 3. Results

### 3.1. Vertical distributions of soil particle compositions

Fig. 2 shows the vertical distributions of the soil particle compositions (sand, silt, and clay contents) at the sampling sites. Clearly, the soil particle compositions all vertically exhibited fluctuating trends at

all of the sampling sites. This is because the Loess Plateau was formed by 37 climate cycles and it comprises different loess-paleosol layers, thereby accounting for the fluctuating trends in the soil particle composition (Ding et al., 1989).

Table 1 shows the descriptive statistics obtained for the soil particle compositions. Clearly, the proportion of coarser particles (sand content) increased among the sampling sites from south to north, whereas the proportion of finer particles (clay content) decreased. The CV was used as an index to represent the overall variation in the parameters. At the sampling sites, the sand contents exhibited moderate variation, the silt contents exhibited weak variation (except at Shenmu), and the clay contents exhibited moderate variation, where they followed the order of: CV sand > CV clay > CV silt. Zhao et al. (2016) determined the PSDs of soils (0–500 cm) in the Loess Plateau region of China and also found that the CV values were highest for the sand content and lowest for the silt content.

### 3.2. Fractal dimensions of PSD

#### 3.2.1. Single fractal dimension of PSD

The ranges of the D values at the five sampling sites comprising Yangling, Changwu, Fuxian, Ansai, and Shenmu from south to north were 2.73–2.88, 2.66–2.90, 2.63–2.89, 2.57–2.87, and 2.67–2.86, respectively, and they all exhibited weak variation (Table 2). Table 4 shows the relationships between the D values and the sand, silt, and clay contents based on the total soil samples. The D value had significant positive relationships with the clay and silt contents, but a significant negative relationship with the sand content. These results are consistent with those reported in previous studies (Gao et al., 2014; Li et al., 2018; Fu et al., 2012), which also showed that the D value had a strong positive linear relationship with the sand content but a negative linear relationship with the sand content.

#### 3.2.2. Multifractal dimension of PSD

Fig. 3 shows the generalized dimension spectra obtained for samples at different depths in Changwu. In order to avoid presenting an excessive amount of data for the five sites, we selected Changwu as a representative site. Clearly, the generalized dimension spectra had a typical sigmoid shape and the range of the left D(q) value ( $-10 < q < 0$ ) was wider than that of the right value ( $0 < q < 10$ ). These results are consistent with previous findings (Peng et al., 2014; Qi et al., 2014; Rodríguez-Lado and Lado, 2017). In addition, the amplitude of the variation differed among samples and particularly for the left branches, thereby indicating that the soil fractal structure varied among samples, especially for the sparse area of PSD ( $q < 0$ ).

We obtained several parameters from the generalized dimension spectra, i.e.,  $D_0$ ,  $D_1$ ,  $D_2$ ,  $D_1/D_2$ , and  $\Delta D$  (Table 3 and 4). The mean  $D_0$  values tended to increase from south to north among the sampling sites ( $P < 0.05$ ), thereby indicating that the particle size range became wider from south to north. The  $D_1$  values were highest at Ansai and Shenmu sites, and those at the other sites did not differ significantly ( $P > 0.05$ ). Thus, the PSDs at Shenmu and Ansai had lower concentrations, whereas the PSDs at other sites had higher concentrations. The  $D_2$  values of five sites were similar ( $P < 0.05$ ), thereby indicating the measurement intervals for the soil particle size were similar.  $D_0/D_1$  was used to quantify the degree of dispersion for the PSD, where a value of  $D_0/D_1$  close to 1 indicates that the soil particles are mainly distributed in dense areas, whereas values close to 0 shows that the soil particles are mainly distributed in sparse areas (Su et al., 2018). The mean  $D_0/D_1$  values at all five sites were close to 1, and thus the PSDs at the five sampling sites were mainly dense. The  $\Delta D$  value was highest at Ansai and lowest at Yangling. Thus, the overall evenness of the soil PSD was lowest at Ansai but highest at Yangling.

The singularity spectra ( $\alpha$ - $f(\alpha)$ ) function was used to quantify the complexity and irregularity of the soil PSD. Fig. 4 shows the singularity spectra obtained for the samples from Changwu site of five sites.

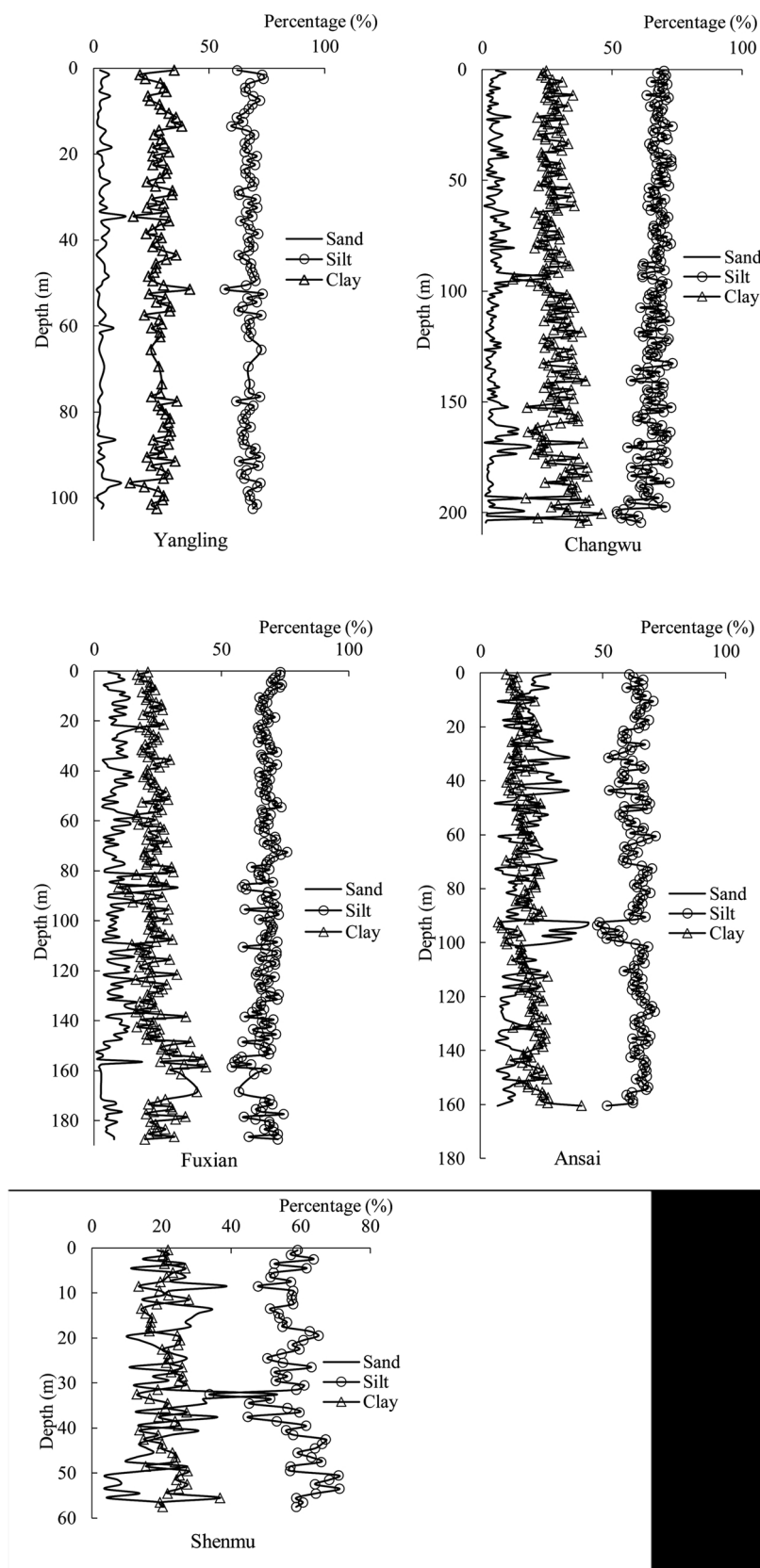


Fig. 2. Vertical distributions of soil compositions at the sampling sites.

**Table 1**  
Descriptive statistics for the soil particle compositions and D values.

Site	No.	Variable	Min	Max	Mean	SD	CV
Yangling	94	Sand	1.44	13.94	3.92	2.12	0.54
		Silt	56.86	73.54	67.27	3.08	0.05
		Clay	15.92	41.68	28.81	4.3	0.15
Changwu	204	Sand	0.89	25.86	5.33	3.91	0.73
		Silt	51.81	73.13	66.37	4.17	0.06
		Clay	11.79	46.03	28.3	5.48	0.19
Fuxian	178	Sand	0.78	32.15	8.88	4.72	0.53
		Silt	54.09	75.89	67.26	3.83	0.06
		Clay	9.69	44.03	23.86	5.23	0.22
Ansai	160	Sand	6.31	44	18.09	7.87	0.43
		Silt	47.75	71.4	63.32	4.59	0.07
		Clay	7.42	41.33	18.6	4.87	0.26
Shenmu	58	Sand	3.68	53.16	20.59	9.19	0.45
		Silt	33.81	71.23	57.76	6.54	0.11
		Clay	13.03	36.93	21.65	4.44	0.21

No., number; Min, minimum; Max, maximum; SD, standard deviation; CV, coefficient of variation

**Table 2**  
Descriptive statistics for the fractal dimensions of the particle size distributions at the five sites.

Site	Variable	Min	Max	Mean	SD	CV
Yangling	D value	2.73	2.88	2.82	0.03	0.01
	R2	0.76	0.90	0.79	0.02	0.02
Changwu	D value	2.66	2.90	2.82	0.03	0.01
	R2	0.75	0.89	0.80	0.02	0.03
Fuxian	D value	2.63	2.89	2.79	0.04	0.01
	R2	0.73	0.87	0.81	0.02	0.03
Ansai	D value	2.57	2.87	2.74	0.05	0.02
	R2	0.79	0.88	0.84	0.02	0.02
Shenmu	D value	2.67	2.86	2.77	0.04	0.01
	R2	0.78	0.94	0.85	0.03	0.03

Min, minimum; Max, maximum; SD, standard deviation; CV, coefficient of variation

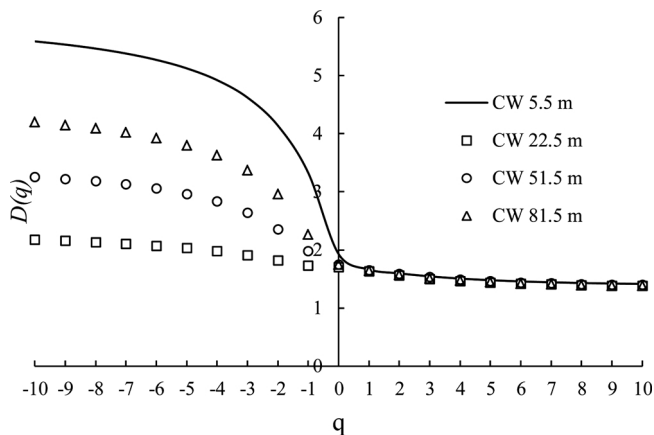


**Fig. 3.** Generalized dimension spectra for selected soil particle size distributions (Changwu).

**Table 3**  
Multifractal characteristic parameters for particle size distributions at different sites.

Sites	D <sub>0</sub>	D <sub>1</sub>	D <sub>2</sub>	ΔD	D <sub>1</sub> /D <sub>0</sub>	Δα	Δf
Yangling	1.808 ± 0.102a	1.64 ± 0.023b	1.568 ± 0.029b	2.894 ± 1.151a	0.91 ± 0.044a	3.388 ± 1.263a	0.936 ± 0.307a
Changwu	1.852 ± 0.126b	1.646 ± 0.035b	1.575 ± 0.042b	3.079 ± 1.27a	0.892 ± 0.052b	3.599 ± 1.382a	0.918 ± 0.323a
Fuxian	1.867 ± 0.117b	1.638 ± 0.041b	1.565 ± 0.048bc	3.032 ± 1.15a	0.88 ± 0.049c	3.547 ± 1.256a	0.891 ± 0.334a
Ansai	1.916 ± 0.084c	1.676 ± 0.057a	1.576 ± 0.093a	3.185 ± 0.993a	0.84 ± 0.049d	3.701 ± 1.104a	1.117 ± 0.409b
Shenmu	1.957 ± 0.057d	1.683 ± 0.053a	1.585 ± 0.069c	3.088 ± 0.84a	0.86 ± 0.031e	3.605 ± 0.932a	1.095 ± 0.399b

Clearly, the singularity spectra had asymmetric shapes and the samples differed in terms of their asymmetry. We also obtained two parameters from the singularity spectra: Δα and Δf. Δα is used to describe the local variability characteristic of the PSD, where a larger Δα indicates a more uneven PSD. There were no obvious trends in the Δα values, but the lowest was at Yangling and the highest at Shenmu. Δf represents the characteristic shape of the multifractal spectrum. All of the Δf values were higher than 0 thereby indicating that the shapes of the singularity spectra deviated to the right and larger probability subsets of the soil PSD played dominant roles. In addition, the Δf values were high at Ansai and Shenmu, but low at the other sites. Thus, the density of larger soil particles was much higher at Ansai and Shenmu.

Table 4 shows the correlation coefficients between the multifractal parameters for the soil PSD and the sand, silt, and clay contents. Clearly, the different parameters yielded different results according to the soil particle composition. For example, D<sub>0</sub> had a significant positive relationship with the sand content and a negative relationship with the silt and clay contents, whereas D<sub>1</sub> had a significant negative relationship with the sand and silt contents and a significant positive relationship with the clay contents. In addition, there were no significant differences between Δα, ΔD, and the soil particle compositions.

#### 4. Discussion

##### 4.1. Effects of the PSD in the Loess Plateau region on multifractal parameters

The Loess Plateau was formed by the deposition of wind-blown dust. This dust debris was initially transported from the northwest area of the Loess Plateau by the force of wind. During this transportation process, the coarser particles were deposited first and the finer particles last, where the latter could have been transported to distant areas (southwest of the Loess Plateau area) (Liu, 1965). Therefore, the particles are increasingly finer from the northwest to the southeast of the region, with a decreasing trend in the sand content but an increasing trend in the clay content. Due to the unique trend of dust debris, D<sub>0</sub> representing the particle size range tended to increase from south to north, whereas D<sub>0</sub>/D<sub>1</sub> representing the degree of dispersion for the PSD tended to decrease. Correlation analysis also showed that D<sub>0</sub> had a significant positive relationship with the sand content, but negative relationships with the silt and clay contents. D<sub>0</sub>/D<sub>1</sub> had significant positive relationships with the silt and clay content, but a negative relationship with the sand content (Table 4).

Higher D<sub>1</sub> values were determined at Shenmu and Ansai, but there were no significant differences among those at the other sites. The higher sand contents at Shenmu and Ansai compared with the other sites (Table 1) may have been related to the more dispersed PSDs at Ansai and Shenmu (higher D<sub>1</sub> values). In addition, the higher sand contents at Shenmu and Ansai resulted in higher Δf values, which represent the distribution density of large probability subsets. Yangling had the lowest Δα and ΔD values, whereas Ansai had the highest. Only 94 soil samples were collected at Yangling whereas the numbers of samples obtained from the other sites exceeded 150 (except at Shenmu). Yangling was the southernmost of the five sites with finer particles, and thus the lowest Δα and ΔD values. By contrast, the samples from Ansai had much higher sand contents, and more soil

**Table 4**  
Correlation coefficients obtained between the soil particle size distribution fractal dimensions and soil particle composition.

Variables	D	D <sub>0</sub>	D <sub>1</sub>	D <sub>2</sub>	D <sub>1</sub> /D <sub>0</sub>	ΔD	Δα	Δf	Sand	Silt	Clay
D	1										
D <sub>0</sub>	-0.26**	1									
D <sub>1</sub>	0.462**	0.291**	1								
D <sub>2</sub>	0.664**	0.067	0.915**	1							
D <sub>1</sub> /D <sub>0</sub>	0.491**	-0.893**	0.169**	0.360**	1						
ΔD	-0.028	0.642**	-0.018	-0.050	-0.670**	1					
Δα	-0.032	0.637**	-0.015	-0.049	-0.664**	0.999**	1				
Δf	-0.19**	-0.083*	-0.051	-0.072	0.06	-0.011	0.002	1			
Sand	-0.88**	0.407**	-0.180**	-0.461**	-0.511**	0.036	0.037	0.209**	1		
Silt	0.22**	-0.421**	-0.238**	0.009	0.320**	-0.063	-0.059	-0.116**	-0.635**	1	
Clay	0.96**	-0.190**	0.425**	0.589**	0.405**	0.004	-0.001	-0.177**	-0.785**	0.019	1

Notes: \*significant difference at 0.05 level; \*\*significant difference at 0.01 level

samples were collected compared with Shenmu, and thus the Δα and ΔD values were highest at Ansai.

4.2. Relationships between fractal parameters and soil particle compositions

Many studies have investigated the relationships between the single fractal and multifractal parameters of the soil PSD and soil particle composition. The relationships reported between the single fractal parameters and soil texture are relatively similar, with significant positive correlations with the clay and silt contents, but significant negative correlations with the sand content (Gao et al., 2014; Liu et al.,

2009; Yao et al., 2015). However, different relationships have been reported between the multifractal parameters and soil texture. For example, we found that D<sub>0</sub> had a significant positive relationship with the sand content and a negative relationship with the silt and clay contents, whereas Qi et al. (2018) reported D<sub>0</sub> had a significant negative relationship with the sand content and a positive relationship with the silt and clay contents. Wang et al. (2008) found a significant positive relationship with the sand content and no relationship with the clay content, and Peng et al. (2014) detected a significant positive relationship with clay content but no relationships with the sand and silt contents. The particle size range, concentration of soil particles, and

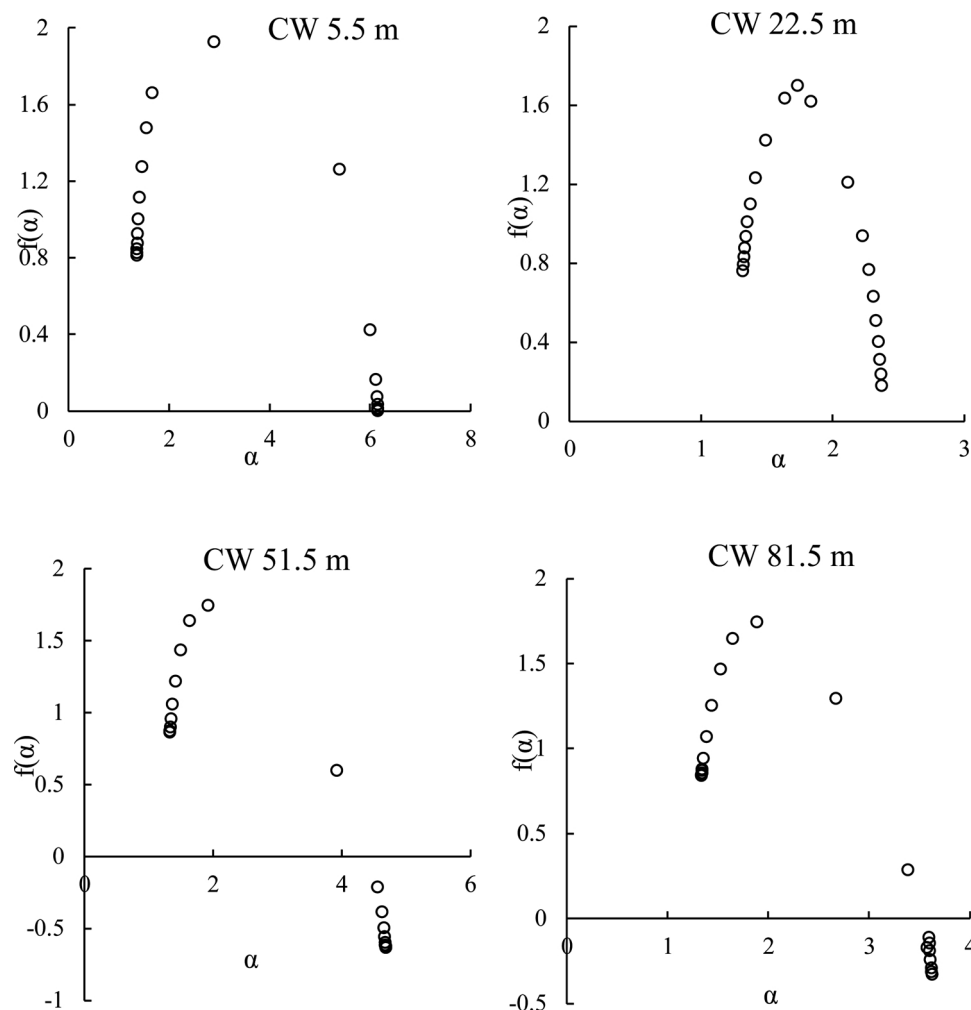


Fig. 4. Singularity spectra for particle size distribution in selected soil samples.

dispersion degree vary among soil samples from different study areas, and thus variable results can be obtained.

## 5. Conclusion

In this study, we employed single fractal and multifractal theory methods to characterize the PSDs in deep soil profiles using samples from the Loess Plateau region. The results showed that the sand content tended to increase whereas the clay content decreased. The range of the PSD was wider from south to north, and the dispersion degree of the PSD became more discrete. The local variability characteristic was lowest in Yangling and highest in Ansai. The shapes of the singularity spectra deviated to the right and large probability subsets of the soil PSDs played major roles at all sites, but especially at Ansai and Shenmu. Our results provided important insights into the deep soil PSD characteristics on the Loess Plateau.

## Declaration of Competing Interest

No conflicts of interest exist regarding the submission of this manuscript and manuscript has been approved for publication by all of the authors. On behalf of my co-authors, I declare that the work described is original research that has not been published previously and it is not under consideration for publication elsewhere, in whole or in part. All the authors have approved the submitted manuscript.

## Acknowledgments

This study was supported by the Postdoctoral Special Funding (2019TQ0266), the Strategic Priority Research Program of Chinese Academy of Sciences (XDB40000000), and the National Natural Science Foundation of China (41701243). The authors thank the editor and reviewers for their valuable comments and suggestions.

## References

- Ding, Z.L., Liu, D.S., Liu, X.M., Chen, M.Y., An, Z.S., 1989. Climate cycle of 37 times since 2.5 million. *Chin. Sci. Bull.* 34 1494–1494.
- Filgueira, R.R., Fournier, L.L., Cerisola, C.I., Gelati, P., Garcia, M.G., 2006. Particle-size distribution in soils: a critical study of the fractal model validation. *Geoderma* 134, 0–334.
- Fu, Y.L., Zhang, X.C., Wang, J.G., 2012. Fractal dimension of soil particle-size distribution characteristics in dry valley of upper Minjiang river. *Trans. Chin. Soc. Agric. Eng.* 28 (5), 127–132.
- Gao, G.L., Ding, G.D., Zhao, Y.Y., Wu, B., Zhang, Y.Q., Qin, S.G., Bao, Y.F., Yu M.H., Liu Y.D., 2014. Fractal approach to estimating changes in soil properties following the establishment of Caragana korshinskii shelterbelts in Ningxia, NW China. *Ecol. Indic.* 43, 236–243.
- Gui, D.W., Lei, J.Q., Zeng, F.J., Mu, G.J., Zhu, J.T., Hui, W., Qiang, Z., 2009. Characterizing variations in soil particle size distribution in oasis farmlands—a case study of the Cele Oasis. *Mathem. Comput. Model.* 1306–1311.
- Hollis, J.M., Hannam, J., Bellamy, P.H., 2012. Empirically-derived pedotransfer functions for predicting bulk density in European soils. *Eur. J. Soil Sci.* 63, 96–109.
- Huang, G., Zhang, R., 2005. Evaluation of soil water retention curve with the pore-solid fractal model. *Geoderma* 127, 52–61.
- Hwang, S.I., Yun, E.Y., Ro, H.M., 2011. Estimation of soil water retention function based on asymmetry between particle- and pore-size distributions. *Eur. J. Soil Sci.* 62, 195–205.
- Jones, C.A., 1983. Effect of soil texture on critical bulk densities for root growth. *Soil Sci. Soc. Am. J.* 47 (6), 1208–1211.
- Keller, T., Dexter, A.R., 2012. Plastic limits of agricultural soils as functions of soil texture and organic matter content. *Soil Res.* 50 (1), 7–17.
- Li, K., Yang, H.X., Han, X., Xue, L.Y., Lv, Y., Li, J.H., Fu, Z.Y., Li, C.R., Shen, W.X., Guo, H.L., Zhang, Y.K., 2018. Fractal features of soil particle size distributions and their potential as an indicator of Robinia pseudoacacia invasion. *Scientif. Rep.* 8, 7075.
- Liu, D.S., 1965. *The Loess Accumulation in China*. Science Press, Beijing, China (in Chinese).
- Liu, D.S., 1985. *Loess and Environment*. Science Press, Beijing, China (in Chinese).
- Liu, X., Zhang, G.C., Heathman, G.C., Wang, Y.Q., Huang, C.H., 2009. Fractal features of soil particle-size distribution as affected by plant communities in the forested region of Mountain Yimeng. *China. Geoderma* 154 (1), 123–130.
- Liu, Y.P., Tong, J., Li, X.N., 2005. Analysing the silt particles with the Malvern Mastersizer 2000. *Water Conservancy Science & Technology & Economy*.
- Lyu, X.F., Yu, J.B., Zhou, M., Ma, B., Wang, G.M., Zhan, C., Han, G.X., Guan, B., Wu, Y.Z., Li, Y.Z., Wang, D., 2015. Changes of soil particle size distribution in tidal flats in the yellow river delta. *Plos One* 10 (3).
- Minasny, B., Stockmann, U., Hartemink, A.E., McBratney, A.B., 2016. Measuring and Modelling Soil Depth Functions. In: Hartemink, E.A., Minasny, B. (Eds.), *Digital Soil Morphometrics*. Springer, Switzerland, pp. 225–240.
- Miranda, J.G.V., Montero, E., Alves, M.C., Paz González, A., Vidal Vázquez, E., 2006. Multifractal characterization of saporite particle-size distributions after topsoil removal. *Geoderma* 134 (3–4), 373–385.
- Montero, E., 2005. Rényi dimensions analysis of soil particle-size distributions. *Ecol. Model.* 182 (3–4), 305–315.
- Peng, G., Xiang, N., Lv, S., Zhang, G., 2014. Fractal characterization of soil particle-size distribution under different land-use patterns in the Yellow River Delta Wetland in China. *J. Soils Sediments* 14 (6), 1116–1122.
- Qi, F., Zhang, R.H., Liu, X., Niu, Y., Zhang, H.D., Li, H., Li, J., Wang, B.Y., Zhang, G.C., 2018. Soil particle size distribution characteristics of different land-use types in the Funiu mountainous region. *Soil Tillage Res.* 184, 45–51.
- Rodríguez-Lado, L., Lado, M., 2017. Relation between soil forming factors and scaling properties of particle size distributions derived from multifractal analysis in topsoils from Galicia (NW Spain). *Geoderma* 287, 147–156.
- Shi, H., Shao, M.A., 2000. Soil and water loss from the Loess Plateau in China. *J. Arid Environ.* 45, 9–20.
- Su, M., Ding, G.D., Gao, G.L., Zhang, Y., Guo, M.S., 2018. Multi-fractal analysis of soil particle size distribution of Pinus sylvestris var. mongolica plantations in Hulunbeier sandy land. *J. Arid Land Resour. Environ.* 32 (11), 129–135.
- Sun, Z.X., Jiang, Y.Y., Wang, Q.B., Owens, P.R., 2018. A fractal evaluation of particle size distributions in an eolian loess-paleosol sequence and the linkage with pedogenesis. *Catena* 165, 80–91.
- Wang, D., Fu, B.J., Zhao, W.W., Hu, H.F., Wang, Y.F., 2008. Multifractal characteristics of soil particle size distribution under different land-use types on the Loess Plateau, China. *Catena* 72 (1), 29–36.
- Wang, Y., Shao, M.A., Liu, Z., Horton, R., 2013. Regional-scale variation and distribution patterns of soil saturated hydraulic conductivities in surface and subsurface layers in the loessial soils of China. *J. Hydrol.* 487 (2), 13–23.
- Xu, G.C., Li, Z.B., Li, P., 2013. Fractal features of soil particle-size distribution and total soil nitrogen distribution in a typical watershed in the source area of the middle Dan River, China. *Catena* 101 (2), 17–23.
- Yao, X.M., Wang, K.B., Zhou, Z.C., Dang, Z.Z., 2015. Fractal features of soil particles during natural vegetation restoration in Ziwuling region. *Chin. J. Soil Sci.* 46 (6), 1380–1385.
- Zhao, C.L., Shao, M.A., Jia, X.X., Zhang, C.C., 2016. Particle size distribution of soils (0–500cm) in the Loess Plateau, China. *Geoderma Reg.* 7 (3), 251–258.
- Zhu, Y.J., Jia, X.X., Shao, M.A., 2018. Loess thickness variations across the Loess Plateau of China. *Surv. Geophys.* 39 (4), 715–727.